Modelisation and Simulation of Heat and Mass Transfers during Solar Drying of Sewage Sludge with Introduction of Real Climatic Conditions

N. Ben Hassine[1,2†], X. Chesneau[1] and A. H. Laatar[2]

[1] *Laboratory of Mathematics and Physics, University of Perpignan Via Domitia, 52 avenue Paul Alduy 66860 Perpignan Cedex 9, France.*

[2] *Laboratory of Energetics and Thermal and Mass Transfers, Faculty of Sciences of Bizerte, University of Carthage, Jarzouna 7021, Tunisia.*

†*Corresponding Author Email: Benhassinenidhal@gmail.com*

ABSTRACT

Sewage sludge presents a real problem with the urban and industrial expanding. So, the drying technique is indispensable in the sludge treatment process to minimize its volume and its revalorization. For cost and environmental reasons, the solar drying is becoming increasingly attractive for small and medium wastewater treatment plants. Therefore, the aim of this work is the modelisation of solar dryer of residual sludge. The model studied is a rectangular agricultural greenhouse. In the lower part, the sludge (assimilated to a porous medium), acts as an absorber. It is subjected to a forced laminar flow. The transfers in the greenhouse and the porous medium are described respectively by the classical equations of forced convection and the Darcy-Brinkman-Forchheimer model. The implicit finite difference method is used to discretize the governing differential equation. The algebraic systems obtained are solved using the Gauss, Thomas and Gauss-Seidel algorithms. In order to complete the model and to determine the drying rate we associate a model of the sewage sludge drying kinetics. This work is realized with the meteorological data of the Tataouine region in the south of Tunisia. This data have undergone statistical treatment using the Liu and Jordan method. In order to show the advantages of solar drying, we especially studied the various transfer modes, the drying kinetics and the dryer performance.

Keywords: Heat and mass transfers; Forced convection; Solar drying; Sewage sludge; Dryer performance.

NOMENCLATURE

c	mass fraction		x	longitudinal coordinate
C_F	Forchheimer coefficient		X	Water content dry base
Da	Darcy number		y	transverse coordinate
Dh	hydraulic diameter			
Dv	vapor diffusion coefficient		$-\dfrac{dX}{dt}$	drying rate
e	thickness of the sludge			
H	channel height			
Hr	relative humidity		α	thermal diffusivity
k	permeability of porous medium		λ	thermal conductivity
L	channel length		ρ	density
L_v	latent heat of vaporization		ν	kinematic viscosity
Ms	dry mass		φ	porosity of porous medium
Pr	Prandtl number		Ω	vorticity
q	solar radiation density		ψ	stream function
Re	Reynold number		α_s	absorption coefficient of the sludge
Sc	Schmidt number		τ_p	transmittance of the greenhouse
T	temperature			
t	temps		**Subscript**	
u	longitudinal velocity		f	fluid
v	transverse velocity			

p	porous
0	ambient
w	wall

1. INTRODUCTION

For a long time solar drying has been used to dry food products to retain them. This type of drying has the advantage that it is not expensive and it does not harm the environment. In recent decades, this type of drying is again interesting with the high cost of drying and the environmental concerns.

Indeed, the topic of drying has been the subject of several research studies, the first scientific works are those of Sherwood (1929 a, b, 1930). He has studied the mechanism of drying and the evaporation of water from solid materials where he has identified four cases. In two cases the evaporation front is located on the solid surface and in the other two cases the evaporation front moves inside. Afterwards, he has shown that the drying rate is not constant during the process. Then, He has shown that drying process consists of two phases, in the first the drying rate is constant, while during the second phase the drying rate is decreasing. He also noted that the decreasing phase is split into two parts. In another work, Sherwood (1936) proposed a classification of the Drying mode according to the shape of the curve of the drying flux depending on the water content and the concavities orientation.

In order to determine a numerical model of urban sludge drying, Vaxelaire *et al.* (2000), Amadou *et al.* (2006) and Slim (2007) have conducted experimental studies by varying the different operating conditions (temperature, humidity and velocity of the ambient air and solar radiation). For the first work, they have proposed a macroscopic approach in terms of curve of kinetics and drying potential. This approach groups a set of external conditions into a single parameter. In the second work the authors have provided a numerical model of the drying kinetics based on the concept of the characteristic curves. In the third, Slim (2007) has proposed a numerical model of the sludge drying that takes into account the variable climatic conditions.

In their work, Vaxelaire and Puiggali (2002), Tao *et al.* (2006) and Font *et al.* (2011) have focused on the phenomenon of shrinkage, the crack formation and the skin layer. By studying the structure of the sludge they have observed the zigzagging form of the cracks inside the samples and the development of a skin layer during the shrinkage. Also they have concluded that these phenomena have an important influence on the drying rate.

Léonard *et al.* (2005) have studied experimentally the influence of air temperature, velocity and humidity during convective drying of two different sewage sludges. They have shown that the temperature is the main operating parameter affecting the drying kinetics. By interpreting the evolution of drying rate depending on the water content, they have confirmed the extragranular limitations during the drying process.

More recent studies have explored various approaches to solve the problem of convective drying of thin film. Among these approaches, we note REA approach (Reaction Engineering Approach), this engineering approach has been used by Putranto *et al.* (2014). The comparison of the results obtained by this model with experimental data shows its effectiveness. Huang *et al.* (2015 and 2016) have used two models to predict the thin layer sludge drying. These models are the Back-Propagation (BP) and the Generalized Regression Neural Network (GRNN) model. They showed that the BP model is more precise for the prediction of the water content of the sludge, whereas for the prediction of the sludge temperature, they have shown that it is valid for the one or the other of the models according to the operating conditions.

As a result, in this work we propose a modelisation of solar dryer for sewage sludge with variable climatic conditions during the day. The case of sewage sludge drying with the meteorological conditions of the Tataouine region was studied to predict the dryer efficiency and the optimal period of drying in these conditions.

2. PROBLEM POSITION

The Fig. 1 schematically shows the greenhouse made up of a horizontal channel where the upper wall is transparent to the solar radiation. The bottom is a porous medium, which has the characteristics of sewage sludge. This sludge is exposed to a forced laminar flow with a parabolic velocity profile at the temperature T_0, the relative humidity Hr_0, the mass fraction C_0 and the constant pressure P_0 at the inlet.
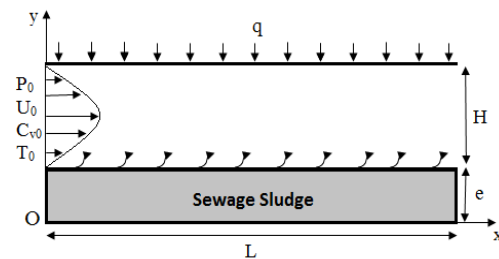

Fig. 1. Geometric configuration.

In order to simplify the problem, the following assumptions are made:

− The transfers are laminar and two-dimensional;

− The fluid is Newtonian and incompressible;

− The viscous dissipation is neglected;

− The Soret and Duffour effects are neglected;

− The Boussinesq approximation is retained;

− The air water vapor mixture is a perfect gas;

− The air-sludge is at local thermodynamic equilibrium;

− The porous medium is isotropic.

3. CONSERVATION EQUATIONS

To generalize the results, the equations are written in dimensionless forms. The variables used to obtain the dimensionless variables are the channel height and the inlet conditions (the velocity, the temperature and the moisture content).

3.1 In the Greenhouse

* Mass conservation

$$\frac{\partial u_f^*}{\partial x^*} + \frac{\partial v_f^*}{\partial y^*} = 0 \qquad (1)$$

* X-momentum conservation

$$\frac{\partial u_f^*}{\partial t^*} + u_f^* \frac{\partial u_f^*}{\partial x^*} + v_f^* \frac{\partial u_f^*}{\partial y^*} = -\frac{\partial P_f^*}{\partial x^*}$$

$$+ \frac{1}{Re_f} \left(\frac{\partial}{\partial x^*} \left(\frac{\partial u_f^*}{\partial x^*} \right) + \frac{\partial}{\partial y^*} \left(\frac{\partial u_f^*}{\partial y^*} \right) \right) \qquad (2)$$

* Y-momentum conservation

$$\frac{\partial v_f^*}{\partial t^*} + u_f^* \frac{\partial v_f^*}{\partial x^*} + v_f^* \frac{\partial v_f^*}{\partial y^*} = -\frac{\partial P_f^*}{\partial y^*}$$

$$+ \frac{1}{Re_f} \left(\frac{\partial}{\partial x^*} \left(\frac{\partial v_f^*}{\partial x^*} \right) + \frac{\partial}{\partial y^*} \left(\frac{\partial v_f^*}{\partial y^*} \right) \right) \qquad (3)$$

* Energy conservation

$$\frac{\partial T_f^*}{\partial t^*} + u_f^* \frac{\partial T_f^*}{\partial x^*} + v_f^* \frac{\partial T_f^*}{\partial y^*} =$$

$$\frac{1}{Pr_f Re_f} \left(\frac{\partial}{\partial x^*} \left(\frac{\partial T_f^*}{\partial x^*} \right) + \frac{\partial}{\partial y^*} \left(\frac{\partial T_f^*}{\partial y^*} \right) \right) \qquad (4)$$

* Species conservation (water vapor)

$$\frac{\partial C_f^*}{\partial t^*} + u_f^* \frac{\partial C_f^*}{\partial x^*} + v_f^* \frac{\partial C_f^*}{\partial y^*} =$$

$$\frac{1}{Sc_f Re_f} \left(\frac{\partial}{\partial x^*} \left(\frac{\partial C_f^*}{\partial x^*} \right) + \frac{\partial}{\partial y^*} \left(\frac{\partial C_f^*}{\partial y^*} \right) \right) \qquad (5)$$

With:

$$Re_f = \frac{H \times U_0}{\nu_f}; Pr_f = \frac{\nu_f}{\alpha_f}; Sc_f = \frac{\nu_f}{D_v}; \alpha_f = \frac{\lambda_f}{\rho_f C_p}$$

Where all the air property $\left(\alpha_f, \lambda_f, \rho_f, D_v, C_p \right)$ are

variable.

3.2 In Porous Medium

In order to ensure the momentum conservation in the porous medium we use the Darcy-Brinkman-Forchheimer model (Swati *et al.,* 2012). In order to overcome the difficulty posed by the boundary conditions to impose on the pressure, the momentum equation is written using the stream function-vorticity formulation (Nogotov *et al.,* 1978). In this formulation the continuity equation is satisfied automatically. So the transfer equations in the porous medium are:

* Stream function equation

$$\frac{\partial^2 \psi}{\partial x^{*2}} + \frac{\partial^2 \psi}{\partial y^{*2}} = -\Omega \qquad (6)$$

* Vorticity equation

$$\frac{1}{\varphi} \frac{\partial \Omega^*}{\partial t^*} + \frac{u_p^*}{\varphi^2} \frac{\partial \Omega^*}{\partial x^*} + \frac{v_p^*}{\varphi^2} \frac{\partial \Omega^*}{\partial y^*} = -\frac{1}{Re_p Da} \Omega^* -$$

$$\frac{C_F}{\sqrt{Da}} \sqrt{u_p^{*2} + v_p^{*2}} \, \Omega^* + \frac{1}{\varphi Re_p} \left(\frac{\partial^2 \Omega^*}{\partial x^{*2}} + \frac{\partial^2 \Omega^*}{\partial y^{*2}} \right) \qquad (7)$$

* Energy conservation

$$\frac{\partial T_p^*}{\partial t^*} + u_p^* \frac{\partial T_p^*}{\partial x^*} + v_p^* \frac{\partial T_p^*}{\partial y^*} =$$

$$\frac{1}{Pr_p Re_p} \left(\frac{\partial}{\partial x^*} \left(\frac{\partial T_p^*}{\partial x^*} \right) + \frac{\partial}{\partial y^*} \left(\frac{\partial T_p^*}{\partial y^*} \right) \right) \qquad (8)$$

With:

$$Re_p = \frac{H \times U_0}{\nu p}; Pr_p = \frac{\nu_p}{\alpha_p}; Da = \frac{k}{H^2}$$

$$u_p^* = \frac{\partial \psi^*}{\partial y^*}; v_p^* = \frac{-\partial \psi^*}{\partial x^*}$$

4. INITIAL AND BOUNDARY CONDITIONS

4.1 Initial Conditions

Initially (t*=0) the temperature, the pressure and the water vapor concentration are uniform in the channel. Inside, the porous medium, the temperature and the water content are also uniform.

4.2 Boundary conditions

For the channel:

* At the inlet

$$u_f^* = 6 \left(y^* - y^{*2} \right); v_f^* = 0; T_f^* = 1; C_f^* = 1$$

* At the outlet

$$\frac{\partial u_f^*}{\partial x^*}=0; \frac{\partial v_f^*}{\partial x^*}=0; \frac{\partial T_f^*}{\partial x^*}=0; \frac{\partial C_f^*}{\partial x^*}=0$$

* At the upper surface

$$u_f^*=0; v_f^*=0; \frac{\partial T_f^*}{\partial y^*}=0; \frac{\partial C_f^*}{\partial y^*}=0$$

For the porous medium:

* At the right and left walls

$$\psi^*=0; \frac{\partial^2\psi^*}{\partial x^{*2}}=-\Omega^*; \frac{\partial T_p^*}{\partial x^*}=0$$

* At the bottom wall

$$\psi^*=0; \frac{\partial^2\psi^*}{\partial y^{*2}}=-\Omega^*; \frac{\partial T_p^*}{\partial y^*}=0$$

For the fluid-porous medium interface:

The longitudinal component of the velocity is obtained by ensuring the continuity of the shear stresses.

$$\mu_f\frac{\partial u_f^*}{\partial y^*}=\mu_p\frac{\partial u_p^*}{\partial y^*}$$

For the stream function and the vorticity, the boundary conditions are:

$$\frac{\partial\psi^*}{\partial y^*}=u_p^*; \frac{-\partial\psi^*}{\partial x^*}=v_p^*; -\Omega^*=\frac{\partial^2\psi^*}{\partial y^{*2}}+\frac{\partial^2\psi^*}{\partial x^{*2}}$$

The heat balance is given us:

$$\frac{H\times\alpha_s\times\tau_p\times q}{T_0}=\lambda_p\left(\frac{\partial T_p^*}{\partial y^*}\right)-\lambda_f\left(\frac{\partial T_f^*}{\partial y^*}\right)-$$

$$\frac{\rho_f\times L_v}{T_0}\frac{D_v}{\left(\frac{1}{C_0}-C_f^*\right)}\frac{\partial C_f^*}{\partial y^*}\Bigg]_{\text{interface}}$$

Assuming that the air-porous media interface is permeable only for the water vapor, the velocity at the interface is written as:

$$v^*=\frac{Ms}{\rho\times S\times U_0}\times\left(\frac{-dX}{dt}\right)_{t^*} \tag{9}$$

Assuming that the air-water vapor mixture is a perfect gas and that the air-porous medium interface is at a local thermodynamic equilibrium. The mass fraction at the interface, C_{fw}^*, can be calculated from:

$$v^*=\frac{-1}{Re_f\,Sc_f}\left(\frac{1}{\frac{1}{C_0}-C_{fw}^*}\right)\left(\frac{\partial C_f^*}{\partial y^*}\right)_w \tag{10}$$

5. METEOROLOGICAL DATA TREATMENT AND DRYING KINETICS MODEL

5.1 Meteorological Data Treatment

Meteorological data are collected using a station installed in a location whose coordinates are: latitude 32° 58'26,76''N, longitude 10° and 29'6,47''E altitude of 210 m (amsl). This station belongs to the EnerMENA project.

Meteorological data have been recorded for a period of 10 years. They have undergone statistical analysis to determine the monthly typical day. Indeed, we used the method of Liu and Jordan (1960). This method supposes that the sky is isotropic and that the intensity of the diffuse sky radiation is assumed to be uniform over the whole sky. It consists to estimate the monthly variation of meteorological variables by a typical day. Every day of the month is the same that this day.

The model equations have been numerically translated using a Fortran program to facilitate calculations.

The solar radiation evolutions during the typical days for the January, .April, July and October months are shown on fig. 2.
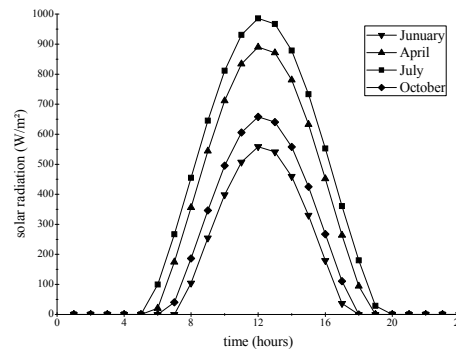
Fig. 2. Solar radiation evolution during the typical days.

5.2 Drying kinetics Model

To determine the drying rate, we adopt a drying kinetics model for the sewage sludge, deduced from the results of Amadou (2006). This model is based on the concept of characteristic curve (Van Meel 1957). The drying rate can be written:

$$\left(-\frac{dX}{dt}\right)_{t^*}=\left(-\frac{dX}{dt}\right)_1\times f(Xr) \tag{11}$$

Where: $\left(-\frac{dX}{dt}\right)_1$ is the constant phase rate.

$f(Xr)=A_1\times Xr+A_2\times Xr^2+A_3\times Xr^3$ is the reduced drying rate.

$Xr=\frac{X-X_{eq}}{X_{cr}-X_{eq}}$ is the reduced water content.

For sewage sludge, the moisture content at equilibrium is given by the following expression (Oswin 1946):

$$X_{eq} = k\left(\frac{Hr}{1-Hr}\right)^n \tag{12}$$

A_1, A_2, A_3, k and n are determined experimentally by Amadou (2007). The values are presented in Table 1.

Table 1 Model parameters

Parameters	Values
A_1	2.37
A_2	-3.30
A_3	1.92
k	0.0938
n	0.484

6. TRANSFERS PARAMETERS AND DRYER EFFICIENCY

6.1 Heat and Mass Transfers Parameters

The solar radiation that reaches the surface of the sludge is decomposed in two modes. One is the sensible heat transfer via the air temperature gradient, Q_s; the other is the latent heat transfer via the water evaporation, Q_l. so the total heat transfer from the surface of the sludge can be expressed as follows:

$$Q = Q_s + Q_l = -\lambda \frac{\partial T}{\partial y} + \rho \times L_v \times v_w \tag{13}$$

The local Nusselt number close to the sludge surface is defined as:

$$Nu_x = Nu_s + Nu_l = \frac{D_h \times Q_s}{\lambda(T_w - T_b)} + \frac{D_h \times Q_l}{\lambda(T_w - T_b)}$$

Where the Nu_s and Nu_l are the local Nusselt numbers for sensible and latent heat transfer, respectively and they are defined in dimensionless form as:

$$Nu_s = \frac{-2}{\left(T_w^* - T_b^*\right)}\frac{\partial T_f^*}{\partial y^*}\Bigg]_w$$

$$Nu_L = \frac{\rho_f \times L_v \times D_h \times U_0}{\lambda \times T_0}\frac{1}{\left(T_w^* - T_b^*\right)}v_w^*$$

The Sherwood number is expressed as:

$$Sh = \frac{D_h(1 - C_w)}{D_v(C_w - C_b)}v_w \tag{14}$$

The dimensionless form is written as:

$$Sh = \frac{U_0 \times D_h\left(\frac{1}{C_0} - C_w^*\right)}{D_v\left(C_w^* - C_b^*\right)}v_w^*$$

Where the subscript b, denotes the bulk quantities. The local bulk temperature T_b and the mass fraction C_b are defined respectively as follows:

$$T_b = \frac{\int_0^L U \times T \times dy}{\int_0^L U \times dy}; C_b = \frac{\int_0^L U \times C \times dy}{\int_0^L U \times dy} \tag{15}$$

6.2 Dryer Efficiency Parameters

The study of the solar dryer efficiency provides a means of assessing just how a dryer operates under certain conditions.

Dryer efficiency is defined as the ratio of energy required to evaporate the water to the energy supplied to the sludge and is calculated from the following mathematical formula:

$$\eta = \frac{Q_{evap}}{Q_{sup}} \tag{16}$$

Where:

$$Q_{evap} = \dot{m} \times L_v$$

$$\dot{m} = Ms \times \left(\frac{dX}{dt}\right)_t \text{ is the mass of water evaporated in}$$

time t.

$$Q_{sup} = S \times \alpha_s \times \tau_p \times q$$

where S is the surface of the sludge.

7. NUMERICAL RESOLUTION AND VALIDATION

7.1 Numerical Resolution

For the two media (fluid and porous), the transfer equations are discretized by using an implicit finite difference method. The numerical resolution is realized by the Gauss and Thomas algorithms in the fluid medium and by the Thomas and Gauss-Seidel algorithms in the porous medium. The considered mesh is regular and rectangular in the two media.

To study the mesh dependence we presented in the Fig. 3 the evolution of the sensible Nusselt number (a) and the evolution of the latent Nusselt number (b) during drying time. The results show that from a nodes number equal to 181 in the X-direction, 181 in the Y-direction for the channel and 41 in the Y-direction for the porous medium, the variations on the evolutions of sensible and latent Nusselt number are minimums. Thereafter, in our simulations we adopt this mesh.

7.2 Validation

The computational code has been validated for the two media. We have compared our results with those of Mohamad (2003) in the case of heat transfer by forced convection in a horizontal channel filled with a porous medium whose walls are maintained at constant temperature (Fig. 4).

For the flow, we have compared our evolution of average Nusselt number with that obtained using the correlation developed by Sieder and Tate (1936) in the case of a laminar flow in a horizontal duct where the walls are at a constant temperature (Fig.

5). For the two cases, the maximum difference does not exceed 4%.
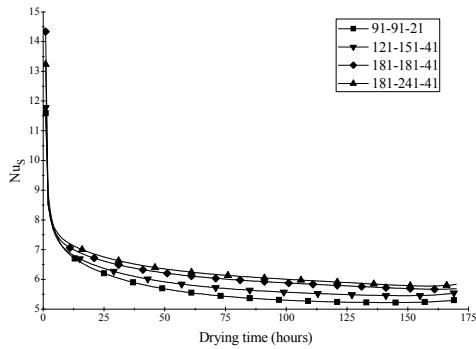
(a)
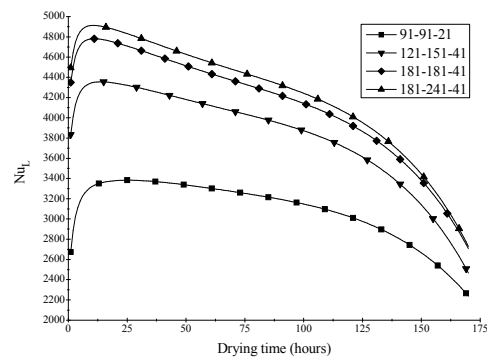
(b)

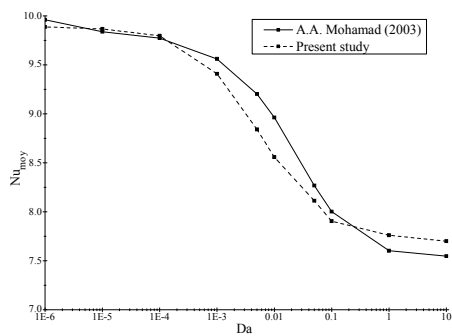**Fig. 3. Mesh sensitivity for sensible Nusselt number (a) and latent Nusselt number (b).**

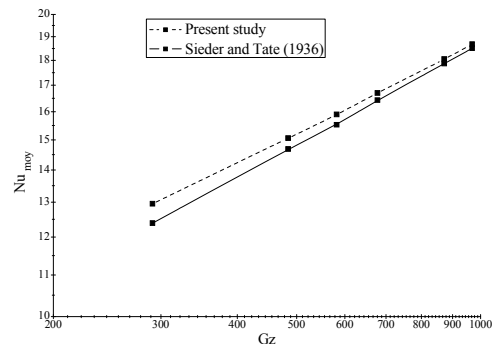**Fig. 4. Nusselt number as a function of Darcy number.**

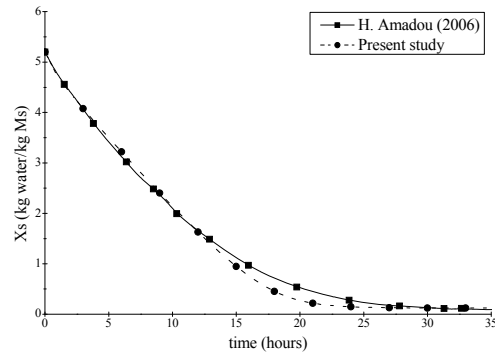**Fig. 5. Nusselt number as a function of Graetz number.**

Fig. 6. Evolution of water content us a function of drying time at T_0=323.68 K, Hr_0=63.59%, U_0=1.79 m/s and q=728 W/m².

We have also validated the model of the drying kinetics used in our simulations. For this, we have compared our results with those of Amadou (2007) in the following conditions; T_0=323.68 K, Hr_0=63.59%, U_0=1.79 m/s and q=728 W/m² (Fig. 6). This comparison shows an acceptable agreement and allows us to validate the used model.

8.   RESULTS AND DISCUSSION

8.1 Heat and Mass Transfers

We have presented one month for each season. So, January is the winter period, April is the spring season, July indicates the summer period and October is the autumn season. The results presented were obtained at 1pm of typical day of months.

The evolution of Nusselt and Sherwood numbers close to the sludge surface are presented on Fig.7, Fig.8 and Fig 9.

On these figures we can see that the mass and heat transfers are more important at the greenhouse inlet. This is due in fact that, at the inlet, the difference between the temperature and mass fraction at the sludge surface and bulk quantities of the air in its vicinity are important (Fig 10). After the entrance zone, the air temperature and humidity increases, so, the temperature and mass fraction gradients close to the sludge surface decreases. It follows that the Nusselt and Sherwood numbers decrease along the greenhouse.
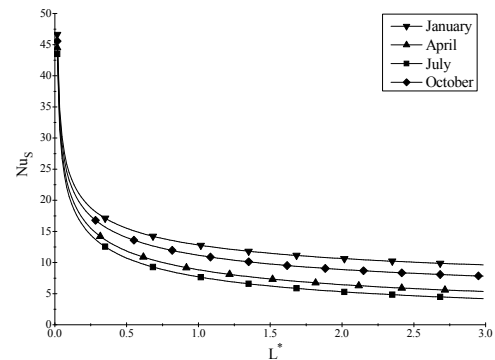

Fig. 7. Local sensible Nusselt number as a function of months close to the sludge surface.
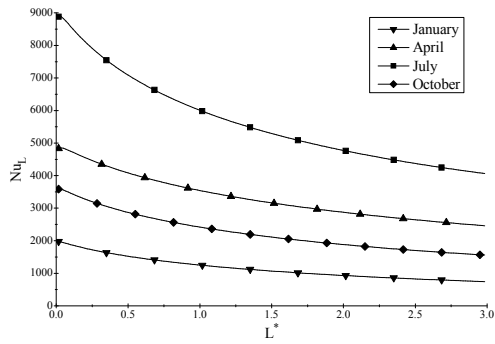
Fig. 8. Local latent Nusselt number as a function of months close to the sludge surface.

We recall that the climatic conditions are optimum during the summer. During this period, the distribution of sensible Nusselt number decreased compared to the winter season evolution, where climatic conditions are at their minimum (Fig. 7). This is due to the fact that in the summer the temperature of the air in the vicinity of the sludge undergoes a larger increase than that of the surface of the sludge (Fig. 10.a). Thereafter, the temperature gradient close to the surface decreases, which implies a decrease of the sensible Nusselt number. We also note that the sensible Nusselt number decreases when going from a cold season to another warmer.
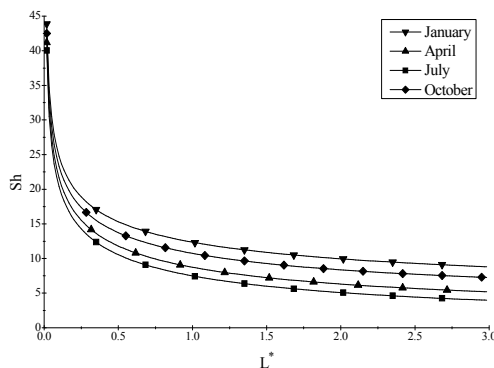
Fig. 9. Local Sherwood number as a function of months close to the sludge surface.

As regards the evolution of the latent Nusselt number we find the inverse phenomenon. The latent Nusselt number increases with the warmer climate. It is at its maximum during the summer and minimum in the winter (Fig. 8). This is due to the mass fraction gradient which increases with climatic conditions. Indeed, with a warm climate, the temperature of the sludge surface is more important than that of a cold climate. This implies an increase of the mass fraction on the sludge surface and thereafter of mass fraction gradient (Fig. 10.b). We note that the heat transfer by latent mode increases from one season to another warmer.

We can also see that the latent Nusselt number is more important than the sensible one, which means the predominance of transfers by latent mode.

Concerning the distribution of the Sherwood number along the sludge surface (Fig. 9), we note that it is similar to that of the sensible Nusselt number. The similarity between the two evolutions can be explained by the fact that for the air the values of Prandtl and Schmidt numbers are very close.
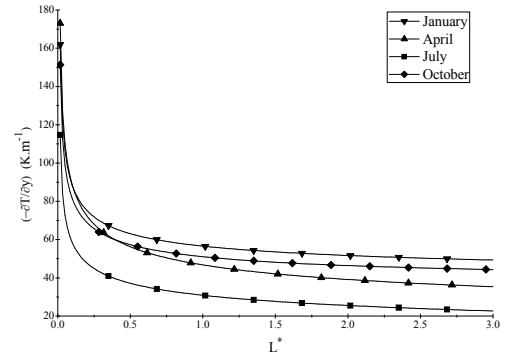
(a)
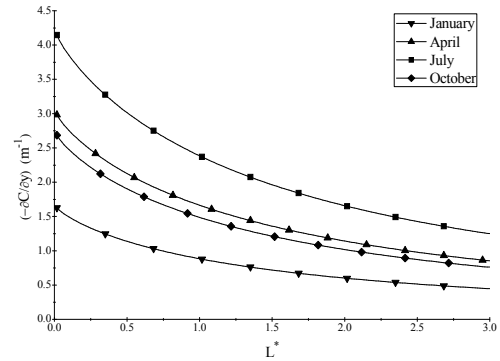
(b)

Fig. 10. Distribution of temperature gradients (a) and mass fraction gradients (b) along the sludge surface.

8.2 Drying kinetics

We present on Fig. 11 the time evolution of the water evaporation rate during the typical day of each month. Firstly we find that the water evaporation rate follows, mainly, the daily evolution of the solar radiation. It is at his maximum or minimum at the same time that the solar radiation. On another hand, it shows as expected, that the water evaporation rate is maximum in July, which corresponds to the summer period, and minimum in January which is representative of the winter season.

During the typical day of January (the winter season), the quantity of water evaporated is equal to 1.49 liter/day/m². This quantity increases for the typical day of April and is equal to 4.69 liter/day/m² (spring season). During the July typical day (the summer period) it reaches a maximum equal to 6.63 liter/day/m². In autumn and during the October typical day, the quantity of water evaporated is lower than that recorded in spring and summer; it is equal to 2.80 liter/day/m².

Table 2 Dryer performance for the 12 typical days

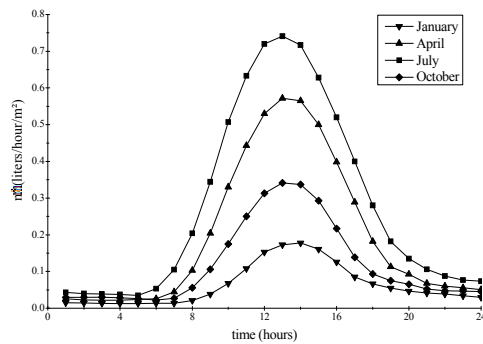| Month	available energy (KWh/m²/day)	supplied energy (KWh/m²/day)	Evaporation energy (KWh/m²/day)	Dryer efficiency (%)
1	3.263	2.629	1.225	46.60
2	3.818	3.186	1.707	53.58
3	5.170	4.180	2.494	59.66
4	6.328	4.816	3.286	68.24
5	7.061	5.665	4.116	72.64
6	7.687	6.087	4.794	78.76
7	7.795	6.442	5.097	79.12
8	6.946	5.883	4.565	77.60
9	5.926	4.805	3.638	75.71
10	4.004	2.925	1.691	57.83
11	3.365	2.436	1.271	52.20
12	3.360	2.395	1.233	51.48

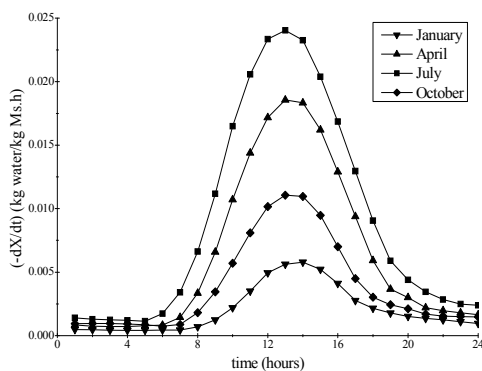**Fig. 11. Time evolution of the average water evaporation rate for various typical days.**

Fig. 12. Time evolution of the average drying rate for various typical days.

As shown in Fig. 12 the drying period has an incontestable effect on the kinetics. As the water evaporation rate, there is a high decrease in the drying rate during the winter period. It increases with a warmer environment and reaches its maximum during the summer. This evolution is identical to that of solar radiation; it is accelerated with his apparition and decreases to a substantially constant value during the night.

8.3 Dryer Efficiency

To be objective in our study we determine the dryer efficiency for 12 typical days. This is enables us to determine the optimal period of drying.

On the Table 2 we have represented the available energy, the supplied energy, the evaporation energy and the dryer efficiency as a function of the typical days. The available solar energy is at its maximum during the summer, specifically in July where it is close to 8 KWh/m²/day, while the minimum is achieved during the winter period when the average value does not exceed 3.5 KWh/m²/day. This is due to the climatic conditions and the duration of sunshine in the Tataouine region that are optimal in the summer.

Also, we note that the evolutions of the supplied energy and the evaporation energy, whatever the month, follow that of the available solar energy. They have a parabolic shape with a maximum recorded around the July.

As expected, the solar efficiency of the greenhouse is also maximum during the summer days. During this period, as we have shown on Fig. 11, the water evaporation rate increases under the effect of climatic conditions. Hence, it follows an increase of drying efficiency.

9. CONCLUSION

In this paper, we present a modelisation of solar dryer of residual sludge. The transfers in the air flow are modeled by the classical Navier-Slokes equations for the forced convection and by the Darcy-Brinkman-Forchheimer model in the sludge considered as a porous medium. The drying kinetics model of sewage sludge is based on the concept of the characteristic curve.

This work is completed by a numerical study of the solar drying of sewage sludge with the climatic

conditions of the Tataouine region in the south of Tunisia. The most significant conclusions of this work are:

– The comparisons between our results and those of the literature shows the validity of our modelisation.

– The heat transfer by latent mode is predominant; the latent Nusselt number is more important than the sensible Nusselt number.

– There is a similarity between the evolution of sensible Nusselt and Sherwood numbers. This similarity is due to the fact that for water vapor the Prandtl and Schmidt numbers are close.

– The water evaporation rate and the drying rate increase with a warmer climate and follow the evolution of the solar radiation.

– The drying efficiency varies under the effect of climatic conditions; it increases when the climatic conditions are optimal and decreases when they are minimal. In fact, the maximum dryer efficiency is recorded during the summer months while the minimum of performance is obtained during the winter.

REFERENCES

Amadou, H. (2007). *Modélisation du Séchage Solaire sous Serre des Boues de Station d'Epuration Urbaines.* Ph. D thesis, ULP Strasbourg 1.

Amadou, H., C. Beck, R. Mose, C Vasile, A. G. Sadowski and J. B. Poulet (2006). Analysis of the Convective Drying of Residual Sludge from the Experiment to the Simulation. *Water Pollution VIII: Modeling, Monitoring and Management* 1, 455-464.

Font, R., M. F. Gomez-Rico and A. Fullana (2011). Skin effect in the heat and mass transfer model for sewage sludge drying. *Separation and Purification Technology* 77, 146-161.

Huang, Y. W. and M. Q. Chen (2015). Artificial neural network modeling of thin layer drying behavior of municipal sewage sludge. *Measurement* 73, 640-648.

Huang, Y. W., M. Q. Chen and L. Jia (2016). Assessment on thermal behavior of municipal sewage sludge thin-layer during hot air forced convective drying. *Applied Thermal Engineering* 96, 209-216.

Léonard, A., S. Blacher, P. Marchot, J. P. Pirard and M. Crine (2005). Convective drying of wastewater sludge: Influence of air temperature, superficial velocity and humidity on the kinetics. *Drying Technology* 23, 1667-1679.

Liu, B. Y. H., R. C. Jordan (1960). The interrelationship and characteristic distribution of direct, diffuse and total radiation. *Solar Energy* 4, 1-19.

Mohamad, A. A. (2003). Heat transfer enhancements in heat exchangers fitted with porous media part I: Constant wall temperature. *International Journal of Thermal Sciences,* 42, 385-395.

Nogotov, E. F., B. M. Berkovsky and W. J. minkowycz (1978). *Application of Numerical Heat Transfer.* Mc Graw-Hill Book Company.

Oswin, C. R. (1946). The Kinetics of Package Life. *International Chemical Industry* 65, 419-421.

Putranto, A. and X. D. Chen (2014). A simple and effective model for modeling of convective drying of sewage sludge: The reaction engineering approach (REA). *Procedia Chemistry* 9, 77-87.

Sherwood, T. K. (1929a). The drying of solids I. *Ind. Eng. Chem.* 21(1), 12-16.

Sherwood, T. K. (1929b). The drying of solids II. *Ind. Eng. Chem.* 21(10), 976-980.

Sherwood, T. K. (1930). The drying of solids III. *Ind. Eng. Chem.* 22(2), 132-136.

Sherwood, T. K. (1936). The air drying of solids. *Trans. Am. Inst. Chem. Engrs.* 32, 150-168.

Sieder, E. N. and G. E. Tate (1936). Heat transfer and pressure drop of liquids in tubes. *Industrial and engineering chemistry* 28(12), 1429-1435

Slim, R., (2007). *Etude et Conception d'un Procédé de Séchage Combiné de Boues de Stations d'Epuration par Energie Solaire et Pompe à Chaleu".* Ph. D. thesis, Ecole des Mines de Paris.

Swati, M., R. D. Prativa, B. Krishnendu and G. C. layek (2012). Forced convective flow and heat transfer over a porous plate in a Darcy-Forchheimer porous medium in presence of radiation. *Meccanica* 47, 153-161.

Tao, T., X. F. Peng and D. J. Lee (2006). Skin layer on thermally dried sludge cake. *Dry. Technol.* 24, 1047-1052.

Van Meel, D. A. (1957). Adiabatic convection batch drying with recirculation of air. *Chemical Engineering Science* 9, 36-44.

Vaxelaire, J. and J. R. Puiggali (2002). Analysis of the drying of residual sludge: from the experiment to the simulation of a belt dryer. *Dry. Technol.* 20(4-5), 989-1008.

Vaxelaire, J., J. M. Bongiovanni, P. Mousques and J. R. Puiggali (2000). Thermal drying of residual sludge. *Water Res.* 34(17), 4318-4323.